J Incl Phenom Macrocycl Chem (2010) 66:285–295
DOI 10.1007/s10847-009-9620-z

ORIGINAL ARTICLE

Liquid crystals based on calix[4]arene Schiff bases

**Ravindra V. Patel · Jayesh G. Panchal ·
V. A. Rana · Shobhana K. Menon**

Received: 17 March 2009 / Accepted: 22 June 2009 / Published online: 7 July 2009

Abstract New liquid crystals based on calix[4]arene Schiff base were prepared by the reaction of tetraamino-calix[4]arene with aldehydes (4-hydroxy benzaldehyde, 2-vanillin, 4-vanillin and 2-hydroxy naphthaldehyde). Dielectric investigations on a magnetically oriented sample forming N, SmA, and SmC phases were carried out. The dielectric constant (ε' and ε") and dielectric loss (tan δ) have been determined as a function of frequency (20 Hz–2 MHz). The synthesized derivatives were purified and characterized by FT-IR, ^{1}H-NMR, ^{13}C-NMR and MALDI-TOF MS. All the synthesized compounds were investigated for liquid crystalline properties using DSC (Differential Scanning Calorimetry), DTA (Differential Thermal Analysis) and POM (Polarizing Optical Microscopy) attached with a hot stage. They generally exhibited nematic and typical fanlike or mosaic texture, which suggest the ordered smectic mesophases. Compounds were found to adopt a specific molecular structure due to the rigid bowl like calix[4]arene core, i.e., a cone-like structure with mesogenic units aligned within the molecule.

Keywords Calix[4]arene Schiff base · Dielectric constant · Mesophases · Thermotropic · Dielectric loss tangent

---

R. V. Patel · J. G. Panchal · S. K. Menon (✉)
Department of Chemistry, School of Sciences, Gujarat University, Ahmedabad 380009, India
e-mail: shobhanamenon07@gmail.com

V. A. Rana
Department of Physics, School of Sciences, Gujarat University, Ahmedabad 380009, India

Introduction

Substances with dielectric constant are widely used in electronic industry [1]. As dielectric interlayers in electronic chips, they strongly increase the speed of propagation of electric impulses and reduce dielectric losses. Electrical properties ferrites are derived from much physical and chemical characterization. The effect of frequency on dielectric offers much valuable information about the localized charge carrier which in turn helps to explain the mechanisms responsible for charge transport phenomena and dielectric behavior. Thermotropic liquid crystals are of great technological importance [2].Terminal groups are one of the important molecular fragments to form liquid crystals. There are different terminal substituent's affianced that are either a small polar substituent (i.e., –CN or –X) or alkyl or alkoxy chains. It is well known that at least one alkyl or alkoxy chain is necessary for the molecular orientation necessary for liquid-crystal phase generation [3]. The interest in synthesis and structural investigation of liquid-crystalline alkyl or alkoxy with calix[4]arene Schiff bases groups in the mesogenic units has considerably increased due to their potential application in the field of nonlinear optics, in optical storage devices and in electro-optical displays. More recently, their applications in light emitting diodes [4] and field effect transistors [5] have also been explored.

Calixarene and their derivatives are attractive compounds for host-guest chemistry and supramolecular chemistry [6] and in the construction of novel molecular architectures [7] because of their tunable and unique three-dimensional structures together with the ease of functionalization. Recently, it has also been used as a building block for liquid crystalline materials [8]. Mesogenic materials with a calix[4]arene central unit were first reported in 1990

[9]. These compounds exhibits columnar mesophases if 12 sufficiently long aliphatic chains are connected to an *exo*-calix[4]arene core [10–12]. Liquid crystalline derivatives, based on *endo*-calix[4]arene has also been reported [13–16]. Recently, liquid crystalline materials of calixarenes have been prepared by the attachment of cyanobiphenyl mesogenic groups to hydroxyl groups on *p-tert*-butylcalix[8]arene and calix[4]resorcinarene, via ester groups having alkyl spacers, which exhibited smectic phases [17]. Similar liquid crystalline phases were showed by octadecyloxy derivative of calix[4]arene [18] and end-functionalized tetra-oligophenylene substituted calix[4]arenes [19]. Our earlier report [20] on the synthesis of crown ether Schiff bases and their promising liquid crystalline properties prompted us to investigate similar properties on calixarene Schiff bases.

In this article we report six new functionalized calix[4]-arene Schiff bases and their liquid crystalline property. Calix[4]arene Schiff bases prepared from various aldehydes (4-hydroxybenzaldehye, 2-vanillin, 4-vanillin, and 2-hydroxynaphthaldehyde) condensed with amino calix[4]arenes substituted with alkyl chains(*n*-butyl, *n*-pentyl and *n*-octyl) at the *para* position through substitution of the hydroxyl group of the *lower rim* of calix[4]arene.All the compounds thus isolated were purified and characterized by FTIR, ^{1}H-NMR, ^{13}C-NMR, and MALDI. Further, compounds were extensively analyzed by using differential scanning calorimetry (DSC) and polarising optical microscopy (POM). Effects of changes in the polar substituents in aldehydes and effect of alkyl chain length on the mesophase were discussed. We have also studied the dielectric properties of calix[4]arene Schiff bases and their electro-optical effect.

Experimental

Apparatus

The FT-IR spectra were recorded as KBr pellet on Bruker TENSOR-27 in the range of 4,000–400 cm^{-1}. Discover BenchMate system-240 V (CEM Corporation) microwave synthesizer was used for synthesis. The MALDI-TOF MS was run on a Micromass TofSpece 2E instrument, using a nitrogen 337 nm laser (4 ns pulse).^{1}H-NMR spectra was scanned on 400 MHz FT-NMR Bruker Avance-400 in the range of 0.5–15 ppm and ^{13}C-NMR spectra was recorded on a Bruker DPX-300 spectrometer using internal standard tetramethylsilane (TMS) and deuterated DMSO as a solvent in the range of 0.5–250 ppm. Transition temperature and enthalpies were scanned in Shimadzu DSC 60, differential scanning calorimeter with a heating rate of 10.0 °C min^{-1} in air and it was calibrated with nitrogen purging at 30 mL min^{-1}. The textures of the mesophases were studied with Leica DMLP polarizing microscope, equipped with a hot stage, Mavotherm 32 temperature display unit and Leica MPS 32 Data back (display unit). Agilent 4980A 005 precision LCR meter (20 Hz–2 MHz over 8610 selectable frequencies) was used for dielectric constant measurements. X-ray diffraction (XRD) experiments were performed on SEIFERT-FPM (XRD7), using Cu Kα 1.5406 Å as the radiation source with 40 kV, 30 mA power and the XRD patterns were recorded at room temperature (25 °C).

Synthesis

p-tert-Butylcalix[4]arene (1) was synthesized by microwave technique developed in our laboratory. The synthesis of the intermediates, debutylated calix[4]arene (2) [21], azocalix[4]arene (3) [22] and tetraaminocalix[4]arene (4) [23] were according to the literature methods.

Microwave-assisted synthesis of 5,11,17,23-tetra-butyl-25,26,27,28 tetrahydroxycalix[4] arene **1**

For the microwave synthesis of **1**, 10 g of *p-tert*-butylphenol was mixed with NaOH (0.05 g, 1.2 mmol) dissolved 0.5 mL of water and 6.2 mL 37% formaldehyde solution and was heated in a Discover BenchMate system-240 V(CEM Corporation) microwave at 300 watt output power for 5 min to give a yellow solid. To this was added 7 mL of diphenyl ether and 1 mL toluene and the mixture was heated at 300 watt output power for 15 min to obtain corresponding calix[4]arene. The purity was checked by TLC and the results of mp, FT-IR, ^{1}H-NMR, ^{13}C-NMR and MS were compared with standard sample.

General synthesis of calix[4]arene Schiff bases, **5**

Tetraaminocalix[4]arene (10 mmol) and aldehydes (40 mmol) (Scheme 1) in anhydrous ethanol (100 mL) was stirred for 2 h under N_2 atmosphere. The yellow precipitate was filtered and recrystallized from ethanol and chloroform.

*Calix[4]arene Schiff base, **5a***

Yield, 2.5 g (83%); m.p. 190 °C. Anal. calc. for $C_{56}H_{44}N_4O_8$: C,74.65; H, 4.92; N, 6.22% Found: C, 74.60; H, 4.93; N, 6.24%. FT-IR(KBr)υ: 3251 cm^{-1}(–OH), 2950 cm^{-1}, 1594 cm^{-1}(CH = N), ^{1}H-NMR (CDCl$_3$) δ 9.5(s, 4H, Ar OH), 9.6 (s, 4H, Ar OH), 8.54 (s, 4H, Ar CH = N), 2.52(s, 8H, CH$_2$), 7.5(d, 16H, ArH), 7.1(m, 8H, ArH). ^{13}C-NMR(CDCl$_3$) 161(CH = N) δ 162, 148, 141, 135, 132, 128, 127, 118 and 116 (Ar C), 13(–CH$_2$–). MALDI-TOF MS(m/z) 901(M) 902(M + 1).

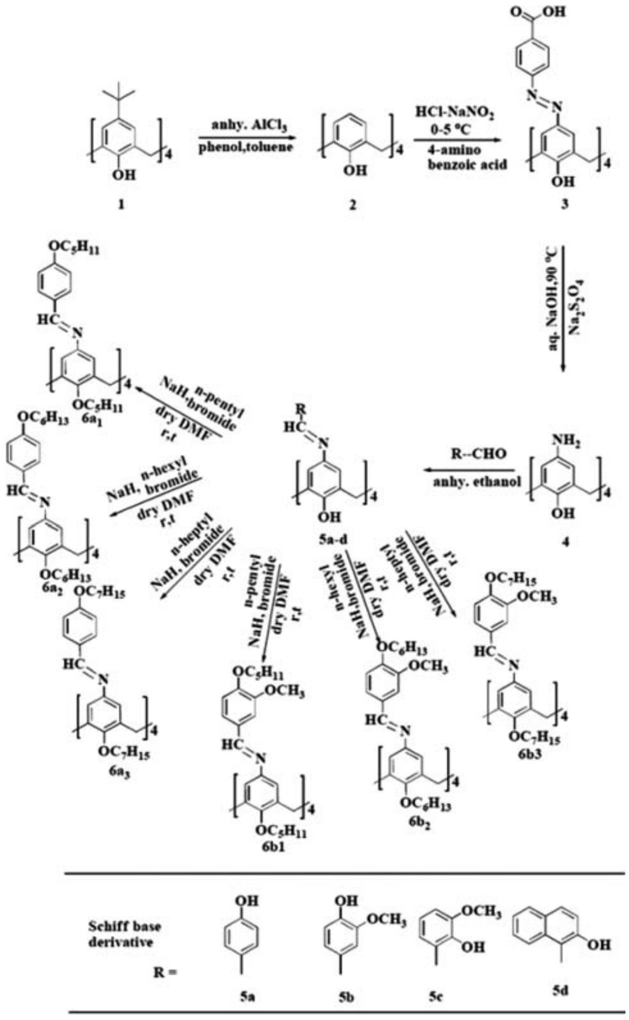

Scheme 1

Calix[4]arene Schiff base, ***5b***

Yield, 2.5 g (83%); m.p. 185 °C. Anal. calc. for $C_{60}H_{52}N_4O_{12}$: C, 70.58; H, 5.13; N, 5.49%. Found: C 70.61: H, 5.12; N, 5.47%. FT-IR(KBr)υ: 3434 cm^{-1}(–OH), 2932 cm^{-1}, 1598 cm^{-1} (CH = N). ^{1}H-NMR ($CDCl_3$) δ 9.3(s, 4H,Ar,OH) 9.55 (s, 4H,Ar OH) 8.54(s, 4H, Ar CH = N) 2.52 (s, 8H, CH_2) 7.15 (m, 12H, ArH) 7(m, 8H, ArH)3.83(s, 12H, CH_3). ^{13}C-NMR($CDCl_3$) δ 160(CH = N), 157, 151, 149, 144.5, 135, 124.8, 118.3, 114.9, 112.1 and 111(Ar C), 56.2(–OCH_3), 13.0(–CH_2–). MALDI-TOF MS (m/z) 1021(M+).

Calix[4]arene Schiff base, ***5c***

Yield, 2.5 g (83%); m.p. 120 °C. Anal. calc. for $C_{60}H_{52}N_4O_{12}$: C, 70.58; H, 5.13; N, 5.49%. Found: C, 70.61; H, 5.12; N, 5.47%. FT-IR (KBr)υ: 3221 cm^{-1}(–OH), 2958 cm^{-1}, 1603 cm^{-1}(CH = N). ^{1}H-NMR ($CDCl_3$) δ 9.5(s, 4H, Ar OH) 13.9 (s, 4H, Ar OH) 8.52 (s, 4H, Ar CH = N) 2.52(s, 8H, CH_2) 7.15 (m, 12H, Ar H)7(m, 8H, ArH)3.83(s, 12H, CH_3). ^{13}C-NMR($CDCl_3$) δ 160(CH = N), 159, 151, 149, 144.7, 128.9, 127.8, 124.1, 119.6, 118.1 and 113(ArC), 56.2(–OCH_3), 13.0(–CH_2–). MALDI-TOF MS(m/z) 1022(M + 1).

Calix[4]arene Schiff base, ***5d***

Yield, 2.5 g (83%); m.p. 205 °C. Anal. calc. for $C_{72}H_{52}N_4O_8$: C, 78.53; H, 4.76; N, 5.09%. Found: C, 78.40; H, 4.79; N, 5.19%. FT-IR (KBr)υ: 3166 cm^{-1}(–OH), 1904 cm^{-1}, 1671(CH = N) cm^{-1}. ^{1}H-NMR ($CDCl_3$) 9.85 (s, 4H, Ar OH) 12.65 (s, 4H, Ar OH) 9.33 (s, 4H, Ar CH = N) 2.58(s, 8H, CH_2) 7.83 (m, 24H, ArH) δ 7.02 (m, 8H, ArH). ^{13}C-NMR($CDCl_3$) δ 153.8(CH = N), 172, 157, 145.1, 135.8, 129.1, 128.0, 127.8, 125.2, 124.9, 122, 118.6 and 116.4(Ar C),13 (–CH_2–). MALDI-TOF MS(m/z) 1103(M+).

General procedure for the substitution of the upper-rim and lower-rim Calix[4]arene compounds **5a** and **5b** [7]

Compound, ***6a₁***

Taken sodium hydride 3.9 g (98.0 mmol) (Scheme 1) and removed paraffin by washing with petroleum ether. Added 80 mL of dry DMF, compound **a** 4.6 gm (9.49 mmol) and 8.17 mL (75.92 mmol) of *n*-butyl bromide and stirred at room temperature for 12 h. Filtered the solid compound. Yield, 90.2%; m.p. 180 °C. Anal. calc. for $C_{96}H_{124}N_4O_8$: C, 78.86; H, 8.55; N, 3.83. Found: C 78.88; H, 8.57; N, 3.81. FT-IR(KBr)υ: 2958 cm^{-1}, 2869 cm^{-1}, 1594 cm^{-1} (CH = N), 1454 cm^{-1}, 1360 cm^{-1}, 1249 cm^{-1}(C–O), 1080 cm^{-1}. ^{1}H-NMR($CDCl_3$) δ 0.88 (t, 24H, CH_3) δ 1.42 (m, 16H, CH_2) δ 8.58(s, 4H, ArCH = N) δ 2.52(s, 8H, CH_2) δ 7.5 (m, 8H, ArH) δ 7.0(m, 16H, ArH) δ 4.12(t, 16H, OCH_2) δ 1.34(m, 32H, CH2). ^{13}C-NMR ($CDCl_3$) δ 160 (CH = N), 161.7, 158, 144.19, 129, 128,117.3, 114.9 and 113.1(ArC), 68.4(–OCH_2–), 35.8, 29, 27, 25.1 and 14.0(alkyl), 13.0(–CH_2–). MALDI-TOF MS(m/z) 1462(M) 1463(M + 1).

In the same way substitution of the hydroxyl group on both upper and lower rim of the Schiff bases **6a₂**, **6a₃**, **6b₁**, **6b₂** and **6b₃** were carried out using *n*-pentyl bromide, *n*-hexyl bromide and, *n*-heptyl bromide.

Compound, ***6a₂***

Yield, 90.2%; m.p. 175 °C. Anal. calc. for $C_{104}H_{140}N_4O_8$: C, 78.86; H, 8.55; N, 3.83%. Found: C, 78.88; H, 8.57; N, 3.81. FT-IR(KBr)υ: 2958 cm^{-1}, 2869 cm^{-1}, 1594 cm^{-1} (CH = N), 1454 cm^{-1}, 1360 cm^{-1}, 1249 cm^{-1} (C–O), 1082 cm^{-1}. ^{1}H-NMR(CDCl$_3$) δ 0.91(t, 24H, CH$_3$) δ 1.42(m, 32H, CH$_2$) δ 8.58(s, 4H, ArCH = N) δ 2.58 (s, 8H, CH$_2$) δ 7.5(m, 8H, ArH) δ 7.1(m, 16H, ArH) δ 4.16(t, 16H, OCH$_2$) δ 1.34(m, 32H, CH$_2$). ^{13}C-NMR(CDCl$_3$) δ 160(CH = N), 161.7, 158, 144.19, 129, 128, 117.3, 114.9 and 113.1(ArC), 68.4(–OCH$_2$–), 35.8, 29, 27, 25.1 and 14.0 (alkyl), 13.0 (–CH$_2$–). MALDI-TOF MS(m/z) 1574(M)1575(M + 1).

Compound, ***6a$_3$***

Yield, 93.2%; m.p. 173 °C. Anal. calc. for $C_{112}H_{156}N_4O_8$: C, 79.01; H, 10.18; N, 3.29%. Found: C, 80.15; H, 9.62%; N, 3.11. FT-IR(KBr)υ: 2958 cm^{-1}, 2927 cm^{-1}, 2868 cm^{-1}, 1590 cm^{-1}(CH = N), 1454 cm^{-1}, 1380 cm^{-1}, 1250 cm^{-1} (C–O), 1120 cm^{-1}, 1082 cm^{-1}. ^{1}H-NMR (CDCl$_3$) δ 0.88 (t, 24H, CH3) δ 1.42 (m, 16H, CH2) 8.58 (s, 4H, Ar CH = N) δ 2.52 (s, 8H, CH$_2$) 7.5 (m, 8H, ArH) δ 7.0 (m, 16H, ArH) 1.30 (m, 32H, CH$_2$) 4.12 (t, 16H, OCH$_2$) δ 1.68 (q, 32H, CH$_2$). ^{13}C-NMR(CDCl$_3$) δ 160(CH = N), 161.7, 158, 145, 129, 128, 127.3, 119.9 and 114.1(ArC), 68.4 (–OCH$_2$–), 31.8, 29, 25.3, 22.1 and 14.1(alkyl), 13.0 (–CH$_2$–). MALDI-TOF MS(m/z) 1685 (M), 1686(M + 1).

Compound, ***6b$_1$***

Yield, 94.8%; m.p. 185 °C. Anal. calc. for $C_{100}H_{132}N_4O_{12}$: C, 75.91; H, 8.41; N, 3.54. Found: C, 75.88; H, 8.45; N, 3.54. FT-IR(KBr)υ: 2957 cm^{-1}, 2871 cm^{-1}, 1594 cm^{-1}(CH = N), 1464 cm^{-1}, 1381 cm^{-1}, 1250 cm^{-1} (C–O), 1211 cm^{-1}, 1086 cm^{-1}, 958 cm^{-1}. ^{1}H-NMR (CDCl$_3$) 0.89(t, 24H, CH$_3$) 8.58 (s, 4H, ArCH = N) 2.52 (s, 8H, CH$_2$) 7.48(m, 12H, ArH) 7.0(m, 8H, ArH) 1.68(q, 16H, CH$_2$) 4.22(t, 16H, OCH$_2$) 1.34(m, 32H, CH$_2$) δ 3.75 (s, 12H, CH$_3$); ^{13}C-NMR(CDCl$_3$) δ 160(CH = N), 152.9, 150.6, 144.7, 129.9, 124.8, 117.3, 114.9, 111.1 and 112(ArC), 69(–OCH$_2$–), 56.2(–OCH$_3$), 29.3, 24.1 and 14.1(alkyl), 13.0(–CH$_2$–). MALDI-TOF MS(m/z) 1582(M + 1).

Compound, ***6b$_2$***

Yield, 94.8%; m.p. 180 °C. Anal. calc. for $C_{108}H_{148}N_4O_{12}$: C, 75.84; H, 9.66; N, 3.28. Found: C, 75.88; H, 8.45; N, 3.5. FT-IR(KBr)υ: 2957 cm^{-1}, 2871 cm^{-1}, 1597 cm^{-1}(CH = N), 1465 cm^{-1}, 1381 cm^{-1}, 1249 cm^{-1} (C–O), 1211 cm^{-1}, 1086 cm^{-1}, cm^{-1}, 958 cm^{-1}. ^{1}H-NMR (CDCl$_3$) 0.89(t, 24H, CH$_3$) 8.58 (s, 4H, Ar CH = N) 2.52(s, 8H, CH$_2$) 7.48 (m, 8H, ArH) δ 7.0(m, 12H, ArH), 1.45 (m, 16H, CH$_2$), 1.68 (q, 16H, CH$_2$) δ 4.22 (t, 16H, OCH$_2$) 1.34 (m, 32H, CH$_2$) δ 3.7 (s, 12H, CH$_3$). ^{13}C-NMR(CDCl$_3$) δ 160(CH = N), 152.9, 150.6, 144.7, 129.9, 124.8, 117.3, 114.9, 111.1 and 112(ArC) 69(–OCH$_2$–), 56.2(–OCH$_2$–),29.3, 24.1, 14.1, 13.0(–OCH$_2$–). MALDI-TOF MS(m/z) 1693(M + 1).

Compound, ***6b$_3$***

Yield, 94.2%; m.p. 176 °C. Anal. calc. for $C_{116}H_{164}N_4O_{12}$: C, 76.44; H, 9.95; N, 3.07. Found: C, 77.60; H, 9.47; N, 2.93. FT-IR(KBr)υ: 2959 cm^{-1}, 2869 cm^{-1}, 1593 cm^{-1} (CH = N), 1454 cm^{-1}, 1380 cm^{-1}, 1249 cm^{-1} (C–O), 1053 cm^{-1}, 961 cm^{-1}. ^{1}H-NMR (CDCl$_3$) 0.88(t, 24H, CH$_3$) 1.45 (m, 16H, CH$_2$) 8.58(s, 4H, ArCH = N) 2.52(s, 8H, CH$_2$) 7.48(m, 12H, ArH) 7.0(m, 8H, ArH) 4.12(t, 16H, OCH$_2$), δ 148(m, 32H, CH$_2$) 1.79(q, 32H, CH$_2$) δ 3.75 (s, 12H, CH$_3$); ^{13}C-NMR(CDCl$_3$) δ 160(CH = N), 159, 150, 144, 129.6, 124.1, 118.3,115.7, 113.1 and 112.2(Ar C), 69.4(–OCH$_2$–), 56.2(–OCH$_3$), 29.6, 29.1, 25.3 and 14.1(alkyl), 13.0 (–CH$_2$–). MALDI-TOF MS(m/z) 1806(M +).

Results and discussion

Synthesis

Microwave synthesis of *p-tert*-butylcalix[4]arene was carried out for the first time by base-catalysed condensation of *p*-substituted phenol and formaldehyde with an improvement of yield to 90–95%.

The synthesis run under microwave irradiation, require only 5–10 mL of solvent as compared to 250–300 mL required for conventional heating method and are radically fast with reaction accomplished within 15–20 min or less with significant increase in the yield. The calix[4]arene derivative (Scheme 2) was prepared by irradiating phenol and formaldehyde mixture by microwave. The preparation of azo calixarenes by three different multi step routes was reported by Taniguchi and coworkers in 1989. The most convenient route involved azo coupling of calixarenes with *p*-carboxybenzenediazonium chloride and reduction of the azo derivatives (aqueous alkaline medium) with sodium dithionite. This compound can also be prepared by first nitrating calixarene and then carrying out reduction by Raney-Ni and hydrazine hydrate but by this route yields were low. On the other hand, product obtained by reduction of dye was in good yield and reaction was accomplished in a rather short span of time. Condensation of teraamino derivative with various aldehydes such as 4-hydroxy benzaldehyde, 2-vanillin, 4-vanillin and 2-hydroxy napthaldehyde gave respective Schiff bases. Substitution of the hydroxyl group on both *upper* and *lower rim* of the Schiff bases **6a$_1$–6a$_3$**, and **6b$_1$–6b$_3$** were carried out using *n*-pentyl bromide, *n*-hexyl bromide and, *n*-heptyl bromide. The introductions of four long alkoxyl group on the *lower rim* of calix[4]arenes locks the macrocycle in cone conformation. This conformation was exclusively achieved by alkylating *lower rim* hydroxyl groups in DMF at room temperature using NaH to impart template effect. In the

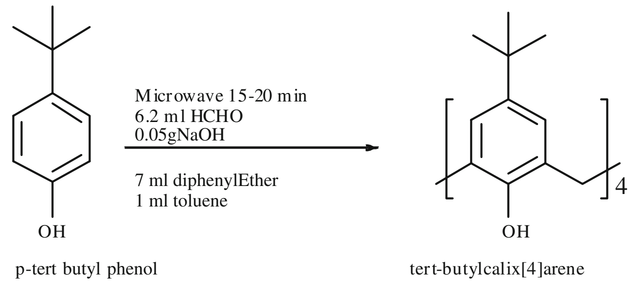

Scheme 2

present investigation, calix[4]arene based Schiff bases showing liquid crystalline property is reported for the first time as compared to different liquid crystalline compounds of calixarene reported earlier.

Physical characterization

All the calix[4]arene Schiff bases thus obtained are found to be thermally stable. Spectroscopic methods (FTIR, ^{1}H-NMR and MALDI-TOF-MS) have been employed to elucidate the structures of the compounds (**5a–5d**, **6a$_1$–6a$_3$** and **6b$_1$–6b$_3$**). FTIR data show that the investigated bonds, which can be assigned to the stretching of imine (C = N) of all compounds were observed at the frequencies of 1,590 to 1,671 cm^{-1}. The bands appearing at 3,166 to 3,434 cm^{-1} in the spectra of compounds except **5a**, **5b**, **5c** and **5d** can be ascribed to the presence of hydroxy (–OH) group. Furthermore this bands fully disappears in the IR spectra of **6a$_{1-3}$** and **6b$_{1-3}$** that indicate absence of hydroxyl (–OH) groups in the compound. Ether bands corresponding to C–O stretching appears at 1,080 to 1,381 cm^{-1}.

^{1}H-NMR data of all the compounds showed that a peak due to the presence of azomethine proton (CH = N) was observable at the chemical shift $\delta = 8.52$ ppm to 9.33 ppm. The appearance of a peak within the range of $\delta = 4.12$ ppm to 4.22 ppm is due to the presence of the proton of ether (–OCH$_2$–) groups.

^{13}C-NMR data of all compounds showed a peak due to the presence of azomethine carbon (CH = N) observable at

Fig. 1 XRD traces of **6a$_1$–6a$_3$** measured at room temperature

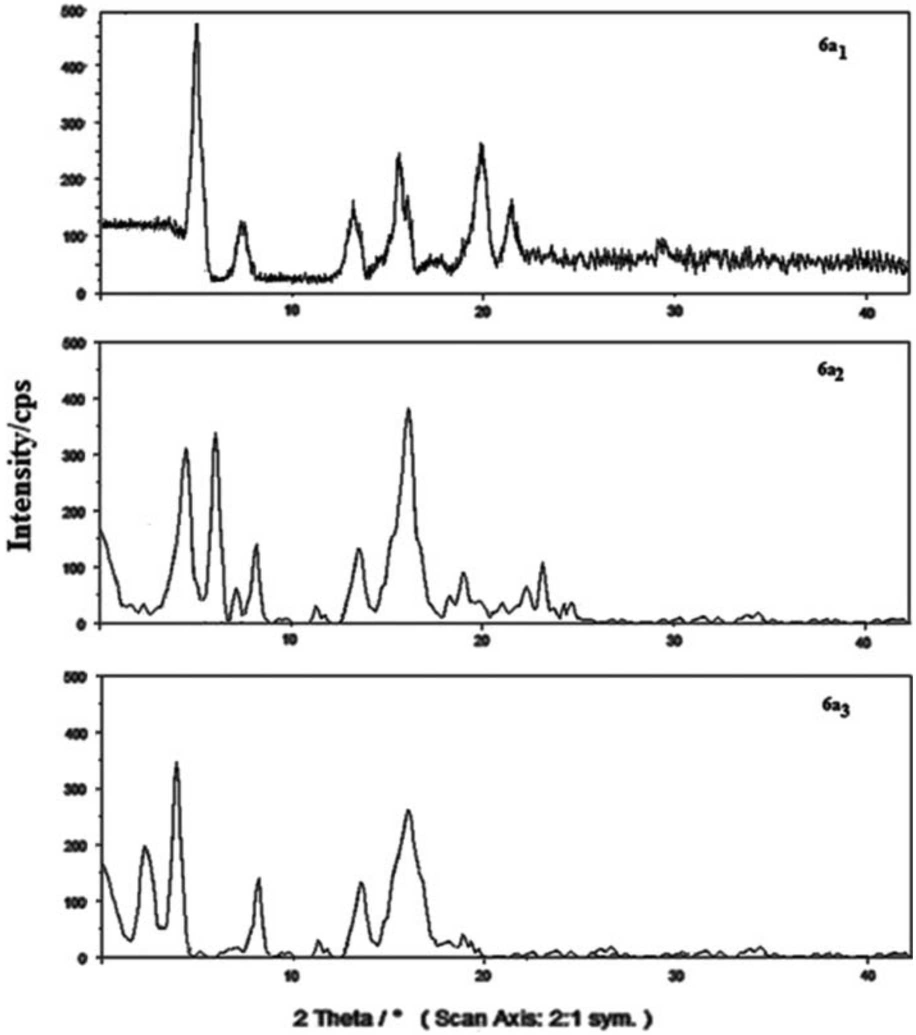

the chemical shift $\delta = 160$ ppm; only compound **5d** showed a peak at $\delta = 153.8$ ppm. The aromatic carbon showed peaks observable at $\delta = 171$–111.3 ppm; aliphatic carbon chain at $\delta = 69.4$–14.1 ppm and methylene bridge carbon showed peak at $\delta = 13.0$ ppm.

The formulations and molecular structure of compounds given in Scheme 2 (**5a–5d**, **6a$_1$–6a$_3$** and **6b$_1$–6b$_3$**) are also supported by the data obtained from MALDI-TOF MS and microanalysis, where in the percentage of C, H and N from the analysis conform the calculated values.

X-ray diffraction measurements

The PXRD pattern of the sample indicated some reflections for small and wide angle areas as illustrated in Figs. 1 and 2 for compounds **6a$_1$–6a$_3$** and **6b$_1$–6b$_3$**. A sharp, low angle peak ($2\theta = 5$–6”), a mid angle region peak ($2\theta = 8$–9”) and a broad region feature at high angle ($2\theta = 19$–22”). The X-ray data show that the position of the small angle reflections depends linearly on the length of the aliphatic chains. The reflections for the small angle area correspond to a smectic layer structure. The d-spacings of the reflections observed for **6a$_3$** at 2 $\theta = 5.56$, 6.39 and 7.4 are 1.4, 1.38 and 1.19 nm while for **6b$_3$** $2\theta = 5.30$, 6.39 and 11.99

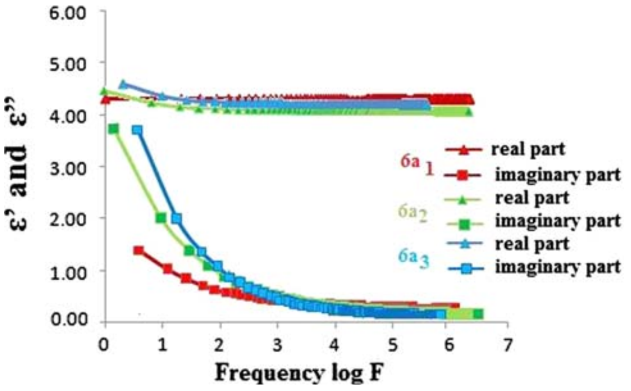

Fig. 3 Variation of dielectric constant with log frequency of compound **6a$_{1–3}$**

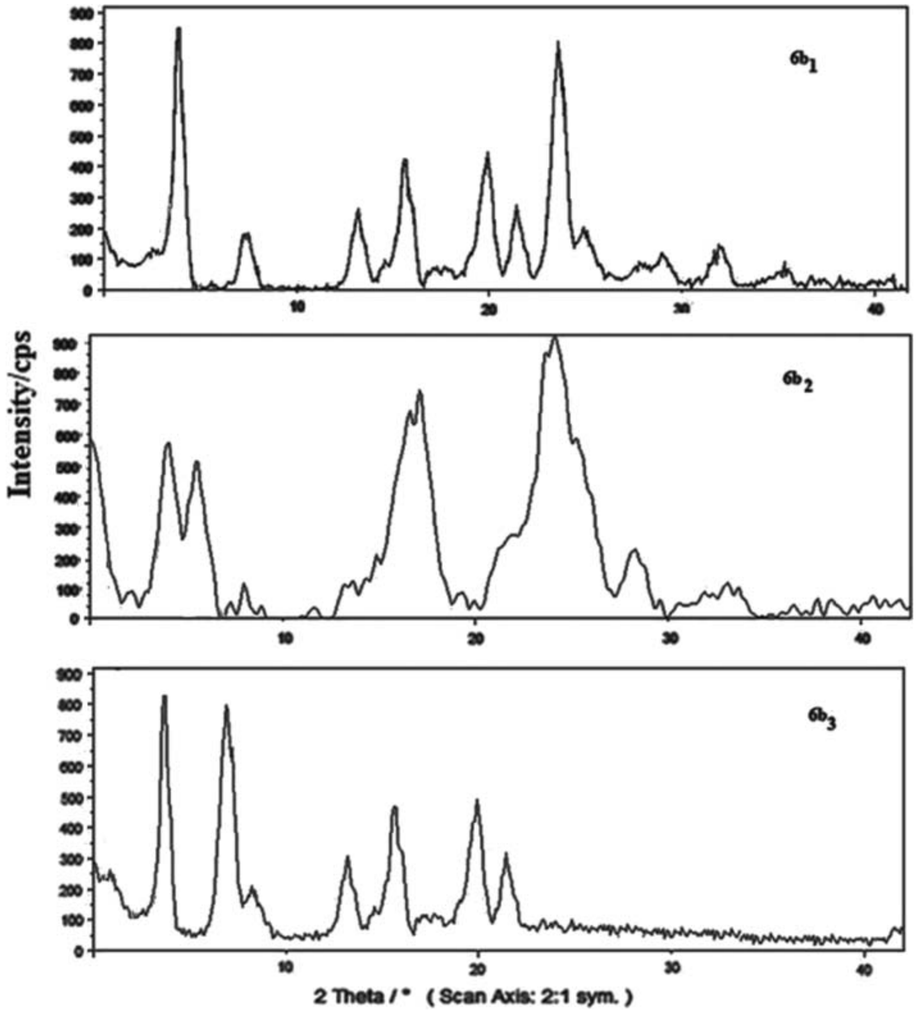

Fig. 2 XRD traces of **6b$_1$–6b$_3$** measured at room temperature

are 1.59, 1.38 and 0.70, respectively, and are associated with first, second and third reflections. The reflections for the wide angle area suggest a highly ordered smectic phases [17].

Dielectric constant studies

Dielectric investigations were carried out in the frequency range from 20 Hz to 2 MHz using Agilent 4980A 005 precision LCR meter. The variation of dielectric permittivity at different frequencies of 20 Hz and 2 MHz is depicted. Variation in real part and imaginary part of complex permittivity of dilute solution of **6a$_{1–3}$** (Fig. 3) and **6b$_{1–3}$** was recorded in chloroform.

From the Fig. 3 it can be seen that at very low frequency dielectric loss (ε' and ε") is high and it decreases with increase in the frequency. High value of dielectric loss at very low frequency is due to the electrode polarization

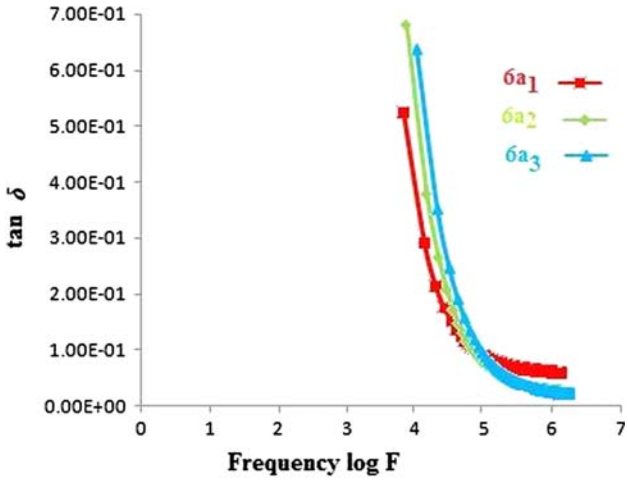

Fig. 4 The dielectric loss tangents of compound **6a$_{1–3}$**

Table 1 Melting point (DTA) of calix[4]arene Schiff bases, **5a–d**

Compound name	m.p. °C
5a	190
5b	185
5c	120
5d	205

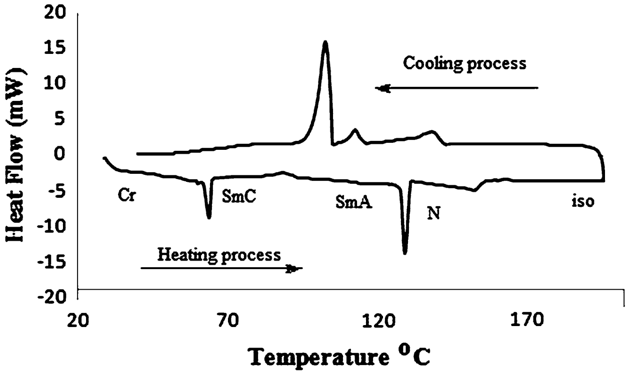

Fig. 5 DSC thermograms for the heating and cooling run at scanning of 10 °C min^{-1} compound **6a$_3$**

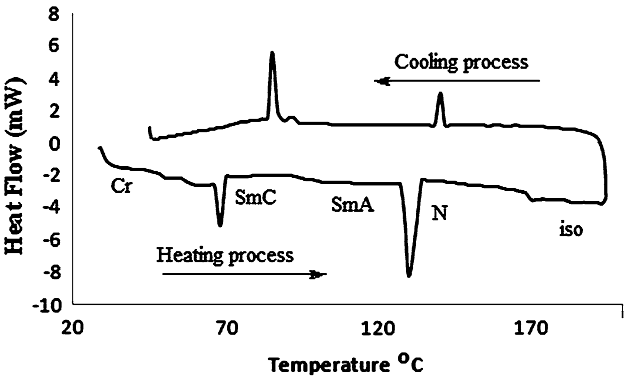

Fig. 6 DSC thermograms for the heating and cooling run at scanning of 10 °C min^{-1} compound **6b$_3$**

Table 2 Transition temperatures observed by means of polarized optical microscopy, Thermal transition data in first heating run of DSC Phase transitions (°C) and corresponding enthalpy changes (J g^{-1})

Compound	Transition	Temperature (°C)	ΔT/°C	ΔH (J g^{-1})
6a$_1$	Cr–Sm C	078.60	–	051.66
	Sm C–Sm A	094.65	016.05	015.23
	Sm A–N	136.80	042.15	009.43
	N–I	180.03	043.23	021.44
6a$_2$	Cr–Sm C	070.92	–	047.97
	Sm C–Sm A	090.72	019.18	011.43
	Sm A–N	130.48	039.76	008.23
	N–I	175.10	044.62	018.89
6a$_3$	Cr–Sm C	063.18	–	043.54
	Sm C–Sm A	085.42	022.44	009.67
	Sm A–N	128.32	042.90	007.45
	N–I	173.43	045.11	015.80
6b$_1$	Cr–Sm C	084.54	–	055.76
	Sm C–Sm A	102.87	018.33	016.20
	Sm A–N	140.65	037.78	011.65
	N–I	185.65	045.00	027.32
6b$_2$	Cr–Sm C	080.34	–	050.89
	Sm C–Sm A	097.99	017.65	013.11
	Sm A–N	132.71	034.72	009.45
	N–I	180.22	047.51	024.71
6b$_3$	Cr–Sm C	068.03	–	045.73
	Sm C–Sm A	090.32	022.29	011.52
	Sm A–N	130.22	039.90	008.76
	N–I	176.43	046.21	020.54

effect. When an electric field is applied to the materials then the long-range drift of ions and barrier layer formation on the electrode surface results in [24] large values of the relative dielectric function. As the frequency increases the dielectric loss decreases approaching near zero value. This suggests that at this dilution and in the considered frequency range all compounds are loss less. Similarly the dielectric constant values of all compounds remain constant over the considered frequency range of 5.36, 5.49, 5.50 for compounds **6a$_1$–6a$_3$** and 5.38, 5.45, 5.55 for compounds **6b$_1$–6b$_3$**.

The value of the loss tangent obtained in the present work in the range of 10^{-1}–10^{-2} at frequencies from a Hz to MHz. These values of the loss tangent are about three compounds **6a$_1$–6a$_3$** (Fig. 4) orders of magnitude lower than those obtained in ferrites prepared by the conventional method [25].The dielectric loss arises, if the polarization lags behind the altering field and is caused by the presence of structural in homogeneities.

Phase transition behaviour and liquid crystallinity of calix[4]arene Schiff bases

All the recently synthesized calix[4]arene Schiff bases **(5a–5d**, **6a$_1$–6a$_3$** and **6b$_1$–6b$_3$)** were studied for the liquid crystalline properties. Melting points of the synthesized calix[4]arenes Schiff bases are given in Table 1 which were obtained from DTA. The transition from the solid state to the first mesophase is considered as the melting point. The thermal and liquid crystalline behaviour of these compounds was investigated by the combination of differential scanning calorimetry and polarized optical microscopy. Consistently with their mesophase behavior, compounds exhibit two endothermic peaks in the heating and cooling

Fig. 7 POM study of the liquid crystals textures of compound **6a$_3$**

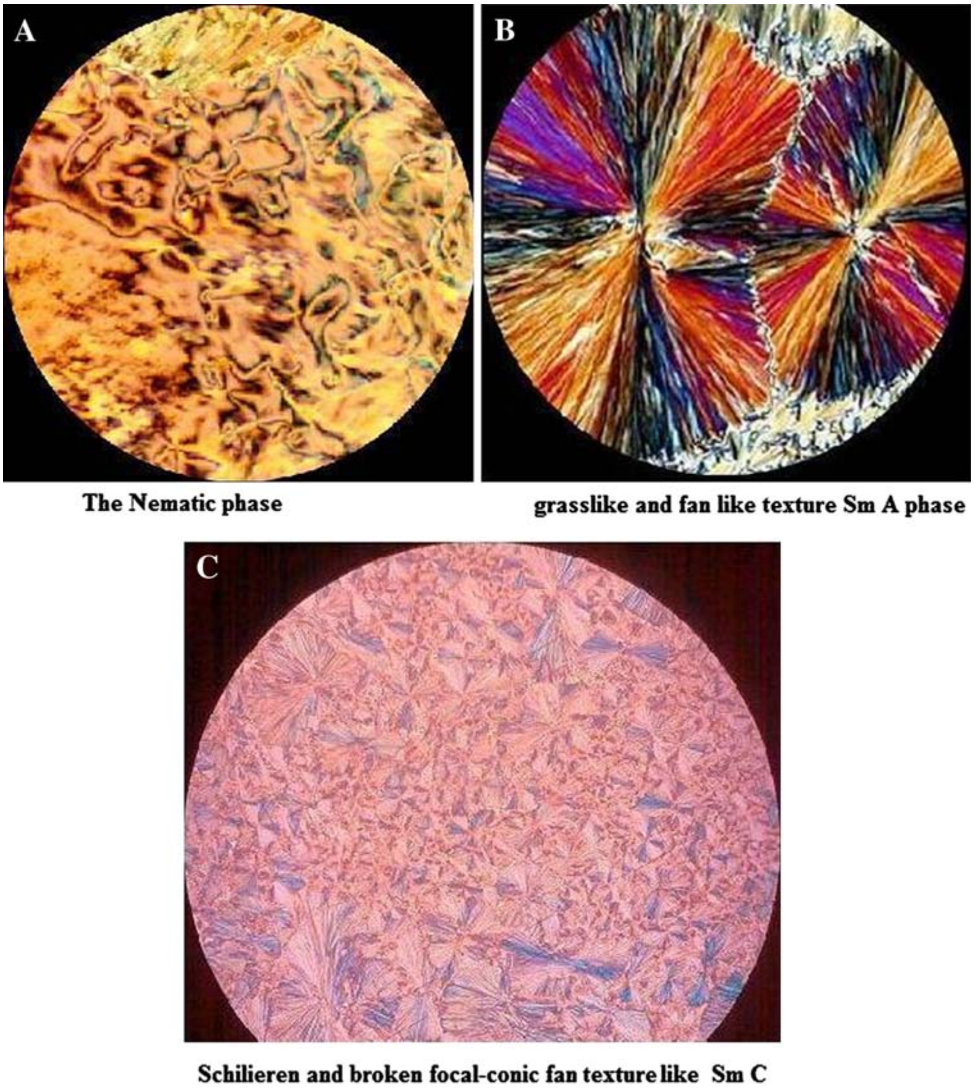

cycles: a small peak at low temperature assigned to the solid to mesophase transition and a large peak at high temperature assigned to the mesophase to liquid transition. The transition from the mesophase to isotropic liquid is not detected in DSC thermograms but is clearly observed in the polarizing optical microscope.

Texture studies

The transition temperatures of the compound **$6a_3$** was determined using a polarizing microscope with a hot-stage. The sequence of phase transitions is given below:

$$\text{Solid} \underset{57^\circ\text{C}}{\overset{63^\circ\text{C}}{\rightleftarrows}} \text{Smectic C} \underset{88^\circ\text{C}}{\overset{90^\circ\text{C}}{\rightleftarrows}} \text{Smectic A} \underset{139^\circ\text{C}}{\overset{140^\circ\text{C}}{\rightleftarrows}} \text{Nematic} \underset{185^\circ\text{C}}{\overset{200^\circ\text{C}}{\rightleftarrows}} \text{Isotropic}$$

The transition temperatures from solid to smectic C, smectic C to smectic A, smectic A to nematic and nematic to isotropic liquid phase are obtained. However, there exists a discrepancy between the experimentally observed and quoted values of the transition temperature between the solid to smectic C and smectic C–smectic A phase. Repeated observations, however, gave the same results. Also, during cooling the phase change from smectic C to solid phase takes place at a lower temperature of 57 °C indicating a super cooled state.

Figures 5 and 6 show DSC study of **$6a_3$** and **$6b_3$**. The DSC thermograms of **$6a_3$** and **$6b_3$** are lower compared to other members. The thermograms show first endothermic peak at 63.18 and 68.03 °C, respectively, while its enthalpy change (ΔH) was approximately 43.54 and 45.73 $\mathrm{Jg^{-1}}$. The second endothermic peak was at 128.32 °C(**$6a_3$**) and 130.22 °C(**$6b_3$**) and its enthalpy change (ΔH) was 7.45 and 8.76 $\mathrm{J\ g^{-1}}$. During cooling process two endothermic peaks were observed at 99.92 and 145.67 °C (Fig. 5) and 102.44 and 136.81 °C (Fig. 6).There was also a small shoulder observed in Fig. 6. From POM investigation it was found that the sample began melting near 190 °C became isotropic at 200 °C. The cooling process showed typical lined texture of the nematic phase after melting. The nematic phase transferred to ordered smectic mesophases.

Fig. 8 POM study of the liquid crystal texture of compound **$6b_3$**

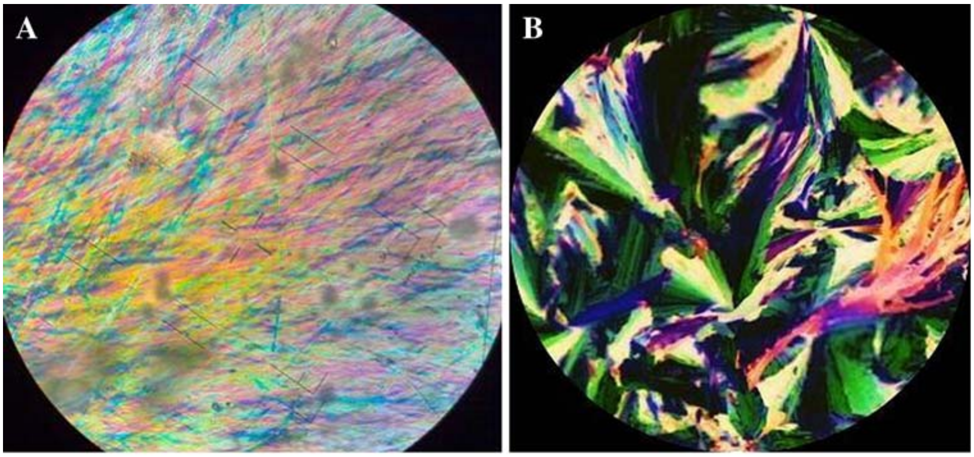

The Nematic phase

mosaic and lancet texture ike Sm A

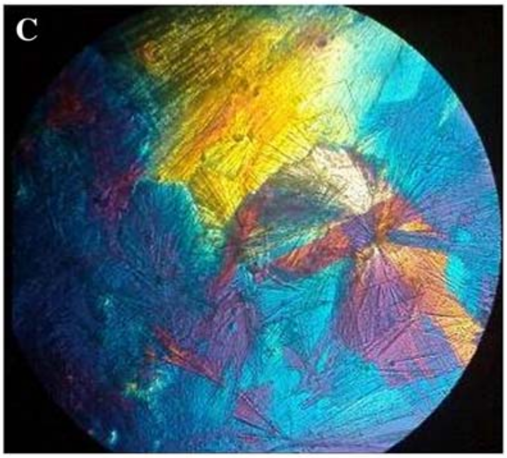

broken focal-conic fan texture like Sm C

Transition temperatures and thermal behaviour of calix[4]arene Schiff bases recorded under the POM and DSC are shown in Table 2. The results show that most of the compounds are mesomorphic in character. The mesophases were identified from their optical textures. Compounds **5c** and **5d** did not show liquid crystal phases which may be due to absence of alkoxy or alkyl chain in the structure. In contrast, a long alkoxy or alkyl group compound **6a$_1$–6a$_3$** and **6b$_1$–6b$_3$** showed nematic and mosaic and lancet and focal-conic fanlike texture which suggest the ordered smectic mesophases. The transition temperature decreases with the increase in the chain length of the alkoxy or alkyl substitution. The order of the change with the transition temperature is heptyl < hexyl < pentyl in both **6a$_1$–a$_3$** and **6b$_1$–b$_3$** and there was not much pronounced effect of polarity in these two series.

Compound **6a$_3$** shows schlieren and broken focal-conic fan texture like Sm C mesophase at 63.18 °C (Fig. 7c) and grass like and fanlike texture Smectic A mesophase at 85.42 °C (Fig. 7b) which on further heating at 128.32 °C transforms into like the nematic mesophase (Fig. 7a) and finally at 173.43 °C into isotropic phase. The textures are taken in cooling condition.

A similar texture is shown by compound **6b$_3$** broken focal-conic fan texture like Smectic C mesophase at 68 .03 °C (Fig. 8c) which changes into mosaic and lancet texture like Smectic A mesophase at 90.32 °C (Fig. 8b). On further heating at 130.22 °C the phase transforms into the nematic (Fig. 8a) and finally at 176.43 °C into isotropic phase. The textures are taken in cooling condition.

Conclusion

All the compounds exhibit thermotropic liquid crystalline behaviour over wide range of temperature and exhibit smectic and nematic phase. The behaviour of the dielectric constant studies shows that as the frequency increases the dielectric loss decreases approaching near zero value. This suggests that at this dilution and in the considered frequency range all compounds are loss less. Substituting the calix[4]arene Schiff base with mesogenic units (e.g., amino, alkoxy, azomethine, ester, etc.) newer compounds with greater mesomorphic range can be designed and hence in the present work molecules have been synthesized by attaching alkane units by ether linkage to the calix[4]arene Schiff base. Most of the compounds exhibit liquid crystalline behaviour on the basis of results obtained from POM and DSC. Also the transition temperatures of the compounds synthesized are very low compared to the reported calix[4]arene liquid crystals and it was shown to decrease substantially by introduction of longer alkoxy chains on both the upper and lower rim. Micrographs show birefringence due to the mesomorphic nature of the compounds. The order of the phase transition: like SmecticA texture-Nematic texture-Isotropic Texture. The compounds are showing mosaic and lancet texture like Smectic A phase, schlieren and broken focal-conic fan texture like Sm C phase, grass like and fan like texture Smectic A phase, broken focal-conic fan texture like Smectic C phase and Nematic phase.

Acknowledgments Financial assistance from UGC, New Delhi is gratefully acknowledged. The authors wish to thank Lucknow for spectral data.

References

1. Maex, K., Baklanov, M.R., Shamiryan, D., Iacopi, F., Brongersma, S.H., Yanovitskaya, Z.S.: Low dielectric constant materials for microelectronics. J. Appl. Phys. **93**, 8793 (2003)
2. Bahadur, B.: Liquid Crystals: Application and Uses, pp. 1–3. World Scientific, Singapore (1995)
3. Castellano, J.A.: RCA Rev. **33**, 296 (1972)
4. Collings, P.J., Hird, M.: Introduction to Liquid Crystals, Chemistry and Physics. Taylor and Francis, London (1997)
5. Seguy, I., Jolina, P., Destruel, P., Farenc, J., Mamy, R., Bock, H., Nguyen, T.P.: Red organic light emitting device made from triphenylene hexaester and perylene tetraester. J. Appl. Phys. **89**, 5442 (2001)
6. Schmidtmende, L., Fechtenkotter, A., Mullen, K., Moons, E., Friend, R.H., MacKenzie, J.D.: Self-organized discotic liquid crystals for high-efficiency organic photovoltaics. Science **293**, 1119 (2001)
7. Gutsche, C.D.: Calixarenes Revisited: Monographs in Supramolecular Chemistry. The Royal Society of Chemistry, London (1998)
8. Nicola, A., Gianluca, A., Yannick, R., Paola, C., Veronica, V., Richard, W., Tao, G., Mohamed, S., Michel, H., Jean-Francois, N.: Electronic properties of oligophenylenevinylene and oligophenyleneethynylene arrays constructed on the upper rim of a calix[4]arene core. New J. Chem. **28**, 1627–1637 (2004)
9. Yonetake, K., Nakayama, T., Ueda, M.: New liquid crystals based on calixarenes. J. Mater. Chem. **11**, 761–767 (2001)
10. Cometti, G., Dalcananle, E., Du Vosel, A., Levelut, A. M.: New bowl-shaped columnar liquid crystals. Chem. Commun. 163–165 (1990)
11. Bonsignore, S., Cometti, G., Dalcanale, E., Du Vosel, A.: New columnar liquid crystals correlation between molecular structure and mesomorphic behaviour. Liq. Cryst. **8**, 639–649 (1990)
12. Abis, L., Arrighi, V., Cometti, G., Dalcanale, E., Du Vose, A.: Deuterium: NMR investigation of a new class of macrocyclic columnar liquid crystal. J. Liq. Cryst. **9**, 277–284 (1991)
13. Budig, H., Diele, S., Paschke, R., Strohi, D., Tschierske, C.: Mesomorphic properties and monolayer behaviour of novel liquid crystalline exo-calix[4]arene derivatives. J. Chem. Soc., Perkin Trans **2**, 1901–1906 (1996)
14. Komori, T., Shinkai, S.: A new class of mesomorphic materials designed from calix[n]arenes. Chem. Lett. **21**, 901–904 (1992)
15. Komori, T., Shinkai, S.: Novel columnar liquid crystals designed from cone-shaped calix[4]arenes. The rigid bowl is essential for the formation of the liquid crystal phase. Chem. Lett. **22**, 1455–1458 (1993)

16. Xu, B., Swager, T.M.: Rigid bowlic liquid crystals based on tungsten-oxo calix[4]arenes: host-guest effects and head-to-tail organization. J. Am. Chem. Soc. **115**, 1159–1160 (1993)
17. Xu, B., Swager, T.M.: Host-guest mesomorphism: cooperative stabilization of a bowlic columnar phase. J. Am. Chem. Soc. **117**, 5011–5012 (1995)
18. Kohmato, S., Someya, Y., Masu, H., Kentaro, Y., Kishikawa, K.: Liquid crystal and crystal structure of octahomotetraoxacalix[4]arenes. J. Org. Chem. **71**, 4509–4515 (2006)
19. Pik Kwan, L., Dongzhong, C., Qingwei, M., Shing Wong, M.: Highly ordered smectic phases from polar calix[4]arene derivatives. Chem. Mater. **18**, 3924–3930 (2006)
20. Menon, S.K., Parikh, V.B.: Synthesis and mesomorphic properties of novel crown ether Schiff bases. Mol. Cryst. Liq. Cryst. **482**, 71–83 (2008)
21. Gutsche, C.D., Iqbal, M., Stewart, D.: Calixarenes. 19. Syntheses procedures for *p-tert*-butylcalix[4]arene. J. Org. Chem. **51**, 742–745 (1986)
22. Deligoz, H.: Synthesis and properties of a series of novel calix[6]arene diazo derivatives. J. Incl. Phenom. Macrocycl. Chem. **43**, 285–289 (2002)
23. Yutaka, M., Toshio, A., Eisaku, N., Hisaji, T.: Syntheses and NMR behavior of calix[4]quinone and calix[4]hydroquinone. J. Org. Chem. **57**, 3658–3662 (1992)
24. Sengwa, R.J., Sankhla, S.: Solvent effect on the dielectric dispersion of poly(vinyl pyrrolidone)-poly(ethyleneglycol) blenas. Colloid Poly. Sci. doi 10.1007/s00396-007-1676-y
25. Laishram, R., Sumitra, P., Sarmaa, H.N.K., Chandra, P.: Influence of Co^{2+} on the electrical and magnetic properties of Li–Sb ferrites. Mater. Lett. **44**, 65 (2000)